Australian Journal of Earth Sciences

ISSN: 0812-0099 (Print) 1440-0952 (Online) Journal homepage: www.tandfonline.com/journals/taje20

Controls on mineralisation in the Sierra Foothills gold province, central California, USA: a GIS-based reconnaissance prospectivity analysis

F. P. Bierlein, H. J. Northover, D. I. Groves, R. J. Goldfarb & E. E. Marsh

To cite this article: F. P. Bierlein, H. J. Northover, D. I. Groves, R. J. Goldfarb & E. E. Marsh (2008) Controls on mineralisation in the Sierra Foothills gold province, central California, USA: a GIS-based reconnaissance prospectivity analysis, Australian Journal of Earth Sciences, 55:1, 61-78, DOI: 10.1080/08120090701581398

To link to this article: https://doi.org/10.1080/08120090701581398

Australian Journal of Earth Sciences (2008) **55**, (61 – 78)

Controls on mineralisation in the Sierra Foothills gold province, central California, USA: a GIS-based reconnaissance prospectivity analysis

F. P. BIERLEIN[1]*, H. J. NORTHOVER[1], D. I. GROVES[1], R. J. GOLDFARB[2] AND E. E. MARSH[2]

[1]*Centre for Exploration Targeting, School of Earth & Geographical Sciences, University of Western Australia, 35 Stirling Highway, Crawley WA 6009, Australia.*
[2]*US Geological Survey, Denver Federal Center, Box 25046, Denver CO 80225, USA.*

The assessment of spatial relationships between the location, abundance and size of orogenic-gold deposits in the highly endowed Sierra Foothills gold province in California, via the combination of field studies and a GIS-based analysis, illustrates the power of such an approach to the characterisation of important parameters of mineral systems, and the prediction of districts likely to host economic mineralisation. Regional- to deposit-scale reconnaissance mapping suggests that deposition of gold-bearing quartz veins occurred in second- and third-order, east-over-west thrusts during regional east – west compression and right-lateral transpression. At the district-scale, significant zones of mineralisation correspond with such transpressional reactivation zones and dilational jogs that developed during the Late Jurassic – Early Cretaceous along the misaligned segments of first-order faults throughout the Sierra Nevada Foothills Metamorphic Belt. Field-based observations and interpretation of GIS data (including solid geology, structural elements, deposit locations, magnetics, gravity) also highlight the importance of structural permeability contrasts, rheological gradients, and variations in fault orientation for localising mineralisation. Although this approach confirms empirical findings and produces promising results at the province scale, enhanced geological, structural, geophysical and geochronological data density is required to generate regionally consistent, high-quality input layers that improve predictive targeting at the goldfield to deposit-scale.

KEY WORDS: California, GIS, orogenic gold, prospectivity analysis, Sierra Foothills, USA.

INTRODUCTION

The Sierra Foothills gold province is host to ~13 000 mines and prospects that are distributed for ~300 km throughout the northern and central Sierra Nevada Foothills Metamorphic Belt in California (Figure 1). The region has yielded >4000 t Au from lode and placer deposits, making it one of the world's premier gold provinces (Lindgren 1895; Knopf 1929; Clark 1992; Böhlke 1999; Walker 2001). Yet, when compared with analogous gold provinces elsewhere, the Californian gold ores remain relatively poorly documented. The structurally controlled deposits are characteristic of orogenic lode-gold deposits worldwide (Goldfarb *et al.* 2001) and are centred on a series of transcrustal curvilinear faults that played a pivotal role in the Late Paleozoic – Early Mesozoic accretionary evolution of the Sierra Nevada Foothills Metamorphic Belt (Landefeld 1988; Edelman & Sharp 1989; Tobisch *et al.* 1989; Miller & Paterson 1991; Kenter 1998; Whitehouse *et al.* 2005; Snow & Scherer 2006). As in most orogenic-gold provinces, the majority of primary production (excluding placer occurrences which account for 40% of total production) has come from a small number of deposits, with the 12 largest lode-gold deposits accounting for almost 60% of the total gold produced in the Sierra Foothills Metamorphic Belt (Figure 2). These deposits are mainly concentrated in the Mother Lode belt, and the Grass Valley and Alleghany districts (Figures 1, 3). The two largest gold lodes are the adjacent Empire and Idaho-Maryland deposits in the Grass Valley district, with a combined production of almost 275 t Au; these are followed by 10 deposits throughout the Sierra Nevada Foothills Metamorphic Belt each with 16 – 50 t Au production, and a further 10 deposits with 10 – 16 t Au production (Table 1; Figure 2).

At a fundamental level, the Sierra Foothills gold province fulfils all criteria required for the generation of an exceptionally well-endowed orogenic-gold province. These criteria include a short (~50 – 70 million years: Snow & Scherer 2006) pre-mineralisation, post-accretionary history of the hosting terranes that implies that a thick subcontinental lithospheric mantle was not

*Corresponding author: bierlein@cyllene.uwa.edu.au

ISSN 0812-0099 print/ISSN 1440-0952 online
DOI: 10.1080/08120090701581398

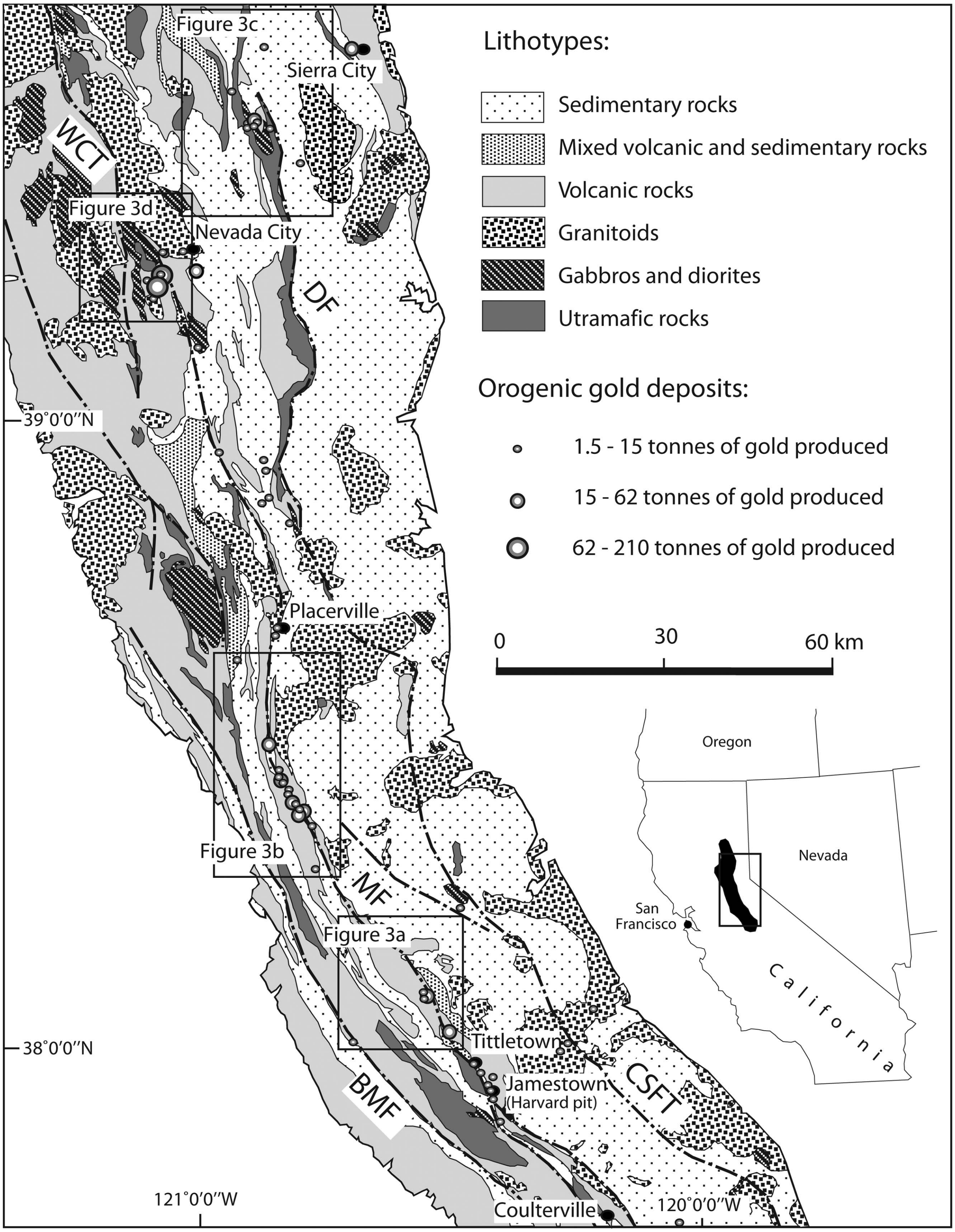

Figure 1 Map of the Sierra Foothills gold province in the northern and central portion of the Sierra Nevada Foothills Metamorphic Belt, showing major lithotypes, selected first-order faults (WCT, Wolf Creek Thrust; MF, Melones Fault; DF, Downieville Fault; BMF, Bear Mountains Fault; CSFT, Calaveras-Shoo Fly Thrust), and location and size of major orogenic-gold deposits (after Clark 1992; Saucedo *et al.* 2000; Snow & Scherer 2006).

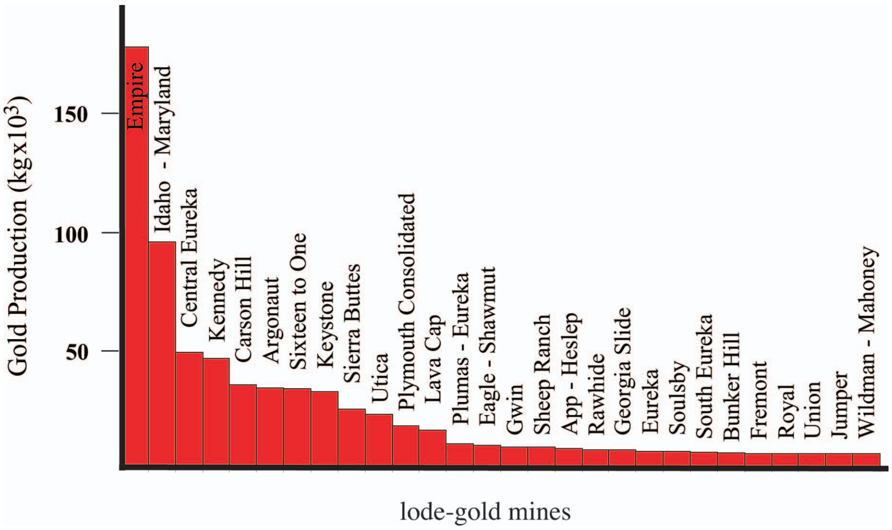

Figure 2 Size distribution of the 30 largest lode-gold deposits in the Sierra Nevada Foothills Metamorphic Belt, based on gold production prior to 1930. Production data from Ferguson & Gannett (1932), Clark & Lydon (1962), Clark (1992), Long *et al.* (1998), Frank (1999) and Anonymous (2006).

developed prior to gold deposition, thin synmineralisation lithosphere (as indicated by contemporaneous magmatism), and the presence of primitive mafic (source) rocks and deep-seated fluid conduits (Bierlein *et al.* 2006a). On the other hand, disparities in size and location of deposits within the gold province are likely to represent significant variations in the degree of conjunction of endowment parameters (Groves *et al.* 2000) that operate at a regional scale. It is these regional-scale parameters that ultimately determine both the size and location of deposits within any given, well- or poorly endowed gold province.

Several studies have applied geometrical and geophysical parameters to systematically test empirical exploration parameters in regional-scale datasets in metallogenically well-endowed provinces (Knox-Robinson & Groves 1997; Brown *et al.* 2000; Groves *et al.* 2000; Knox-Robinson 2000; Bierlein *et al.* 2006b). Although long recognised to host a world-class gold province, no such study has been applied to date to the Sierra Nevada Foothills Metamorphic Belt. In this paper, geological and geophysical characteristics that act as proxies for critical ore deposition parameters in an orogenic-gold province, and aid in the assessment of primary controls on gold mineralisation in the northern and central portions of the Sierra Nevada Foothills Metamorphic Belt, are identified. These parameters are then interpreted within a GIS framework to statistically define the relative importance of the parameters and the relevant empirical relationships between them. The potential power of such an approach lies in its ability to predict the location of well-endowed domains in a gold province.

TECTONIC SETTING AND REGIONAL GEOLOGY

The Sierra Nevada Foothills Metamorphic Belt is part of the North American Cordilleran orogen that extends from Alaska to California and comprises turbiditic terranes, island-arc complexes, and backarc basins accreted to the North American craton (Dilek & Harris 2004). During the Early Paleozoic, the southern part of North America was primarily a passive margin setting. In the Late Paleozoic, oceanic Antler and Sonoma allochthons were thrust over the continental margin. Transition to an accretionary orogen commenced in the Mesozoic, with the Nevadan orogenic event (initiated *ca* 163–152 Ma) marking the final, regionally pervasive deformation in the Sierra Nevada Foothills Metamorphic Belt (Böhlke 1999). The subsequent westward migration of the locus of accretion and underthrusting has been attributed to a fundamental shift in the far-field stress regime (Dilek & Harris 2004). Under this new stress regime, the Sierra Block (accreted terranes and Sierra Nevada Batholith) was uplifted and tilted, with erosion continuing into the Cenozoic (Sharry 1982). The most extensive unroofing has occurred in the southern Sierra, where the deepest parts of the batholith are exposed today. Total erosion in the central and northern Sierra Nevada Foothills Metamorphic Belt has been estimated at between 3 and 12 km (Bateman & Eaton 1967; Ross 1983).

The Sierra Nevada Foothills Metamorphic Belt comprises a diverse collage of Paleozoic and Mesozoic metasedimentary and metavolcanic rocks. Five terranes were progressively accreted from east to west (Northern Sierra and Feather River terranes, Calaveras Complex, Jurassic–Triassic Arc Belt and Middle–Late Jurassic Arc Sequence: Snow & Scherer 2006). These terranes are bounded by a series of transcrustal, curvilinear faults (e.g. Melones Fault, Bear Mountains Fault, Downieville Fault, Calaveras–Shoo Fly Thrust and Wolf Creek Thrust: Figure 1), which themselves comprise tectonic mélanges of medium- to high-grade metamorphic rocks.

Extending almost the entire length of the Sierra Nevada Foothills Metamorphic Belt, both the Melones and Bear Mountain Faults are mid-Jurassic sutures that subsequently defined zones of failure between the accreted terranes (Vernon *et al.* 1989; Barriga *et al.* 1992). The Bear Mountain Fault is made up of a tectonic mélange of serpentinised ultramafic rocks and rare inclusions of high-pressure–high-temperature rocks, including eclogite and garnet amphibolite (Miller & Paterson 1991). In the northern Sierra Nevada Foothills Metamorphic Belt, the Melones Fault comprises a ~3.5 km-wide zone of serpentinite and mélange.

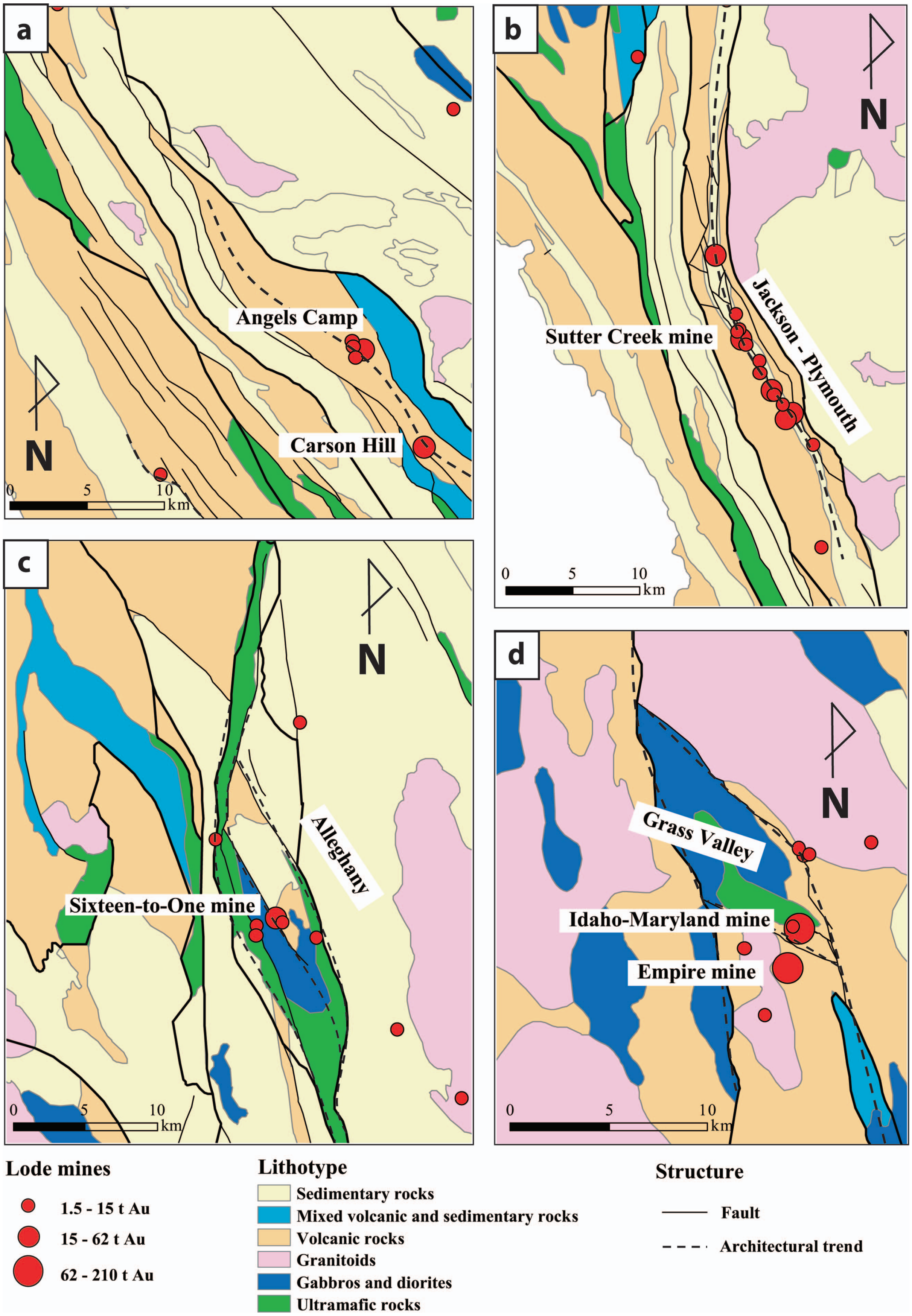

Figure 3 Geological sketch maps illustrating the spatial relationship of major gold districts and first-order faults in the Sierra Nevada Foothills Metamorphic Belt. (a) Angels Camp and Carson Hill. (b) Jackson-Plymouth. (c) Alleghany. (d) Grass Valley. Lithotypes are as shown in Figure 1 (after Clark 1992; Saucedo *et al.* 2000; USGS 2006).

Table 1 Characteristics of the largest 12 orogenic lode-gold deposits in the Sierra Foothills gold province, California.

Mine/deposit	Goldfield	Location (UTM x / y)	Production (t)[a]	Host-rock	Orientation of nearest first-order fault segment	Orientation of nearest lithological contact	Magnetic anomaly signature
Empire	Grass Valley	668757.34, 4341488.31	178.3	Porphyry	160°	146°	Magnetic high
Idaho-Maryland	Grass Valley	669340.26, 4343382.39	96.2	Serpentinite	160°	108°	Magnetic high
Central Eureka	Jackson-Plymouth	692380.25, 4250604.11	49.4	Greenstone & slate	156°	156°	Minor magnetic gradient
Kennedy	Jackson-Plymouth	693927.73, 4248852.23	47	Greenstone & slate	156°	156°	Minor magnetic gradient
Carson Hill	Carson Hill	719698.11, 4210210.96	35.7	Greenstone & slate	146°	160°	Minor magnetic low
Argonaut	Jackson-Plymouth	693404.12, 4248407.85	34.6	Greenstone & slate	156°	156°	Minor magnetic gradient
Sixteen-to-One	Alleghany	685534.50, 4370588.76	34.3	Amphibolite	177°	40°	Strong magnetic gradient
Keystone	Jackson-Plymouth	690080.36, 4254435.77	32.9	Greenstone & slate	156°	156°	Minor magnetic gradient
Sierra Buttes	Sierra City	702470.07, 4383231.26	25.4	Amphibolite	158°	146°	Minor magnetic gradient
Utica	Angels Camp	715821.68, 4216493.05	23.3	Greenstone & amphibolite	125°	150°	Minor magnetic low
Plymouth Consolidated	Plymouth	688131.39, 4260754.08	18.5	Slate	160°	160°	Minor magnetic gradient
Lava Cap	Nevada City	675156.71, 4344004.15	16.5	Slate	193°	88°	Magnetic gradient

[a]In many instances, these figures are rough estimates only: data from Ferguson & Gannett (1932), Clark & Lydon (1962), Clark (1992), Long *et al.* (1998), Frank (1999), and Saucedo *et al.* (2000).

Towards the southern segment of the Sierra Nevada Foothills Metamorphic Belt, the fault narrows to a 1 km-wide mylonite–phyllonite shear. Variations in brittle–ductile features reflect variations in the levels of crustal exposure along the length of the Sierra Nevada Foothills Metamorphic Belt (Landefeld 1988; Paterson & Wainger 1991; Barriga *et al.* 1992). Seismic profiling has correlated the Melones Fault with a prominent regional reflector dipping landward at about 40°, which continues below the Sierra Nevada Batholith and persists to at least mid-crustal levels (Nelson *et al.* 1986). Downdip extension lineations and a C–S cleavage relationship with host-rocks are consistent with the interpretation that the Melones Fault represents an east-over-west thrust that, as indicated by cross-cutting relationships with several *ca* 140 Ma plutons (Sharp 1980), developed a dominantly lateral sense of movement during the Jura-Cretaceous (Paterson & Wainger 1991).

Magmatism in the Sierra Nevada Foothills Metamorphic Belt relates to arc volcanism, with Late Mesozoic to Neogene volcanic rocks distributed within the five terranes. Plutonic rocks are primarily constrained to two magmatic episodes that corresponded to changes in the rate of subduction, subduction dip angle, and obliquity of convergence between the North American and Farallon Plates (Tobisch *et al.* 1995; Dilek & Harris 2004). The first of these periods was in the Late Jurassic, immediately prior to the Nevadan Orogeny, when plutons were intruded at depths of between 20 and 30 km with a general southwest-younging trend across all five terranes of the Sierra Nevada Foothills Metamorphic Belt (Bateman & Eaton 1967; Day & Bickford 2004). The second extensive phase of magmatism in the Cretaceous was related to a change from normal to more oblique-dextral convergence between 105 and 80 Ma (Tobisch *et al.* 1995). This culminated in the emplacement of the massive Sierra Nevada Batholith, a major continental arc located about 20–30 km to the east of the lode deposits.

NORTHERN SIERRA NEVADA AND MOTHER LODE GOLD DEPOSITS

Gold deposits occur along almost the entire length of the Sierra Nevada Foothills Metamorphic Belt, but by far the most productive are those situated in the northern and central portion of the metamorphic belt (Figure 1). Towards its northern termination, the gold-hosting region is as wide as 120 km and includes the Grass Valley, Alleghany, Sierra City and Nevada City districts. By contrast, most of the historically significant districts in the 200 km-long central portion (the Mother Lode Belt) of the Sierra Nevada Foothills Metamorphic Belt occur within a <4 km-wide, north-northwest-trending corridor centred on the Melones Fault. The greatest production there came from the Jackson-Plymouth, Angels Camp, Jamestown, Placerville and Carson Hill districts (Clark 1992). The linear array of deposits and their concentration along major structural trends were first noted by Lindgren (1895). The deposits are sited in variably faulted and sheared, amphibolite- to greenschist-facies lithologies that include serpentinite, granitoids, mafic to felsic volcanic rocks and turbiditic sedimentary rocks. All rocks are metamorphosed, but primary textures and structures are generally well preserved; hence, the prefix 'meta-' is inferred but omitted.

At the deposit scale, there is a close spatial relationship between gold and serpentinised ultramafic bodies. Our reconnaissance-level structural analyses of several of the major gold deposits have confirmed the findings of previous studies (Knopf 1929; Ferguson & Gannett 1932; Coveney 1981; Clark 1992). Multi-phase formation of the lode structures took place in a subhorizontally oriented, east–west far-field stress regime, with compression resulting in reactivation of pre-existing structures in the form of minor east-over-west thrusting. Mineralisation is concentrated in zones of minimum principal stress and dilational structures (Figure 4), including conjugate shears (e.g. Empire deposit, Grass Valley district); granitoid pressure shadows (e.g. Oriental deposit, Alleghany district); dilational jogs linked to flattening of the footwall contact (e.g. Sixteen-to-One deposit, Alleghany district); fault jogs (e.g. Harvard deposit, Jamestown district); and along lithological contacts with pronounced competency gradients (e.g. Idaho-Maryland deposit, Grass Valley district; Sierra Butte deposit, Sierra City district; Sutter Creek deposit, Jackson-Plymouth district; Calaveras Vein, Carson Hill district; Gold Bug deposit, Placerville district). The laminated to massive, stylolitic, braided-ribbon, crack-seal or brecciated quartz (±ankerite–sericite/mariposite–feldspar–chlorite) veins in these deposits vary in thickness from a few millimetres to tens of metres, and can be laterally extensive for several kilometres (Figures 4, 5). Cross-cutting relationships point to a complex evolution of veins, with multiple reactivations, but gold-bearing quartz-vein formation in most deposits is temporally related to a switch from normal-sinistral to dextral transpression, giving rise to the commonly steeply north-plunging ore shoots. For example, the majority of ore shoots comprising gold-bearing quartz veins and 'grey ore' (i.e. greenstone bodies with disseminated auriferous pyrite adjacent to quartz veins: Clark 1992) in the Jackson-Plymouth district have a distinctive and steep northerly plunge when projected on to a long-section plane of the Melones Fault (Figure 6). This steep north plunge of mineralisation could reflect the intersection of bedding planes with the Melones Fault but is best interpreted as a result of dextral-reverse thrusting during vein formation. In view of the north-northwest-trend of the Melones Fault in the Jackson-Plymouth district, such displacement would most likely have occurred during west-southwest–east-northeast compression. This assessment also broadly agrees with the structural interpretation of north–south-trending, 35°E–W-dipping conjugate vein sets in granodiorite at the Empire deposit in the Grass Valley district. The vein-hosted gold in these deposits typically is coarse-grained, with a low abundance of pyrite and arsenopyrite, and with wall-rock alteration characterised by pervasive sericitisation (mariposite), carbonation and chloritisation (Coveney 1981; Weir & Kerrick 1987) (Figure 5e).

Geological, structural and petrographic evidence confirm that quartz veins throughout the belt formed late during the *ca* 150–120 Ma deformation of the Sierra Nevada Foothills Metamorphic Belt (Böhlke 1999). Available Ar–Ar, K–Ar and Rb–Sr age constraints indicate that the majority of gold deposits formed between *ca* 125 and 115 Ma, corresponding to significant gold-mineralising events elsewhere in the Circum-Pacific region (Evans & Bowen 1977; Kistler *et al.* 1983; Böhlke & Kistler 1986; Goldfarb *et al.* 1998). Significantly older, apparent *ca* 140 Ma Ar–Ar and Rb–Sr ages for the Brunswick deposit (Grass Valley district) reported in Böhlke & Kistler (1986) were considered anomalies by these authors, and are also somewhat contradictory to geological and structural evidence for a regionally consistent timing of gold mineralisation.

As in many analogous gold provinces elsewhere, the ultimate source of the gold, and origin of ore-bearing fluids, in the Sierra Nevada Foothills Metamorphic Belt have been debated since Lindgren (1895) first contemplated these aspects. He, as well as Knopf (1929) and Johnston (1940), favoured a magmatic source, in part because of the proximity of gold deposits to the Sierra Nevada Batholith, and their apparent temporal overlap of emplacement. On the basis of fluid-inclusion and stable-isotope studies, Weir & Kerrick (1987) and Nesbitt (1991) proposed an ore-fluid model involving deep circulation of meteoric water, but the significance of the analysed fluids, particularly as to how they related to the gold mineralisation, remained uncertain (Böhlke 1999 and references therein). More recent studies in the Mother Lode, and comparisons with orogenic-gold provinces elsewhere, suggest a metamorphic origin of the vein-forming fluids, with the gold probably derived from suitable source rocks such as ultramafic and mafic rocks of the accreted oceanic and arc terranes (Albers 1981; Böhlke & Kistler 1986; Bierlein *et al.* 1998, 2006a; Böhlke 1999; Goldfarb *et al.* 2001). Stable-isotope (H, N, O) data from hydrothermal micas and auriferous vein material in several major deposits in the Mother Lode Gold Belt also support a

Figure 4 (a) Rock face (looking northeast) in the Carson Hill pit, exposing the phyllite-hosted Calaveras Vein; note bleaching of host rocks on left-hand side of vein, ankeritic alteration halo, and dip-slip striations in centre left of photograph. (b) Steeply east-trending (direction of index finger) dip-slip lineations on sheared footwall-vein contact of the 29 Vein in the Sutter Creek deposit (Jackson-Plymouth district) overprint the pervasive foliation but are themselves overprinted by north-northwest-trending strike-slip striations (approximately horizontal in photograph). (c) Subhorizontal conjugate veins in the 29 Vein in the Sutter Creek deposit. (d) *En échelon* jogs within a set of subhorizontal conjugate shears (dipping gently to the south-southwest and north-northeast) in the Harvard Pit, Jamestown. (e) Subhorizontal conjugate vein sets in outcrop at the McAlpine deposit (Coulterville district). (f) Tightly folded and sheared quartz–gold vein at the contact of pervasively foliated phyllite and serpentinite (dark rock in bottom part of photograph) in the Gold Bug deposit (Placerville district).

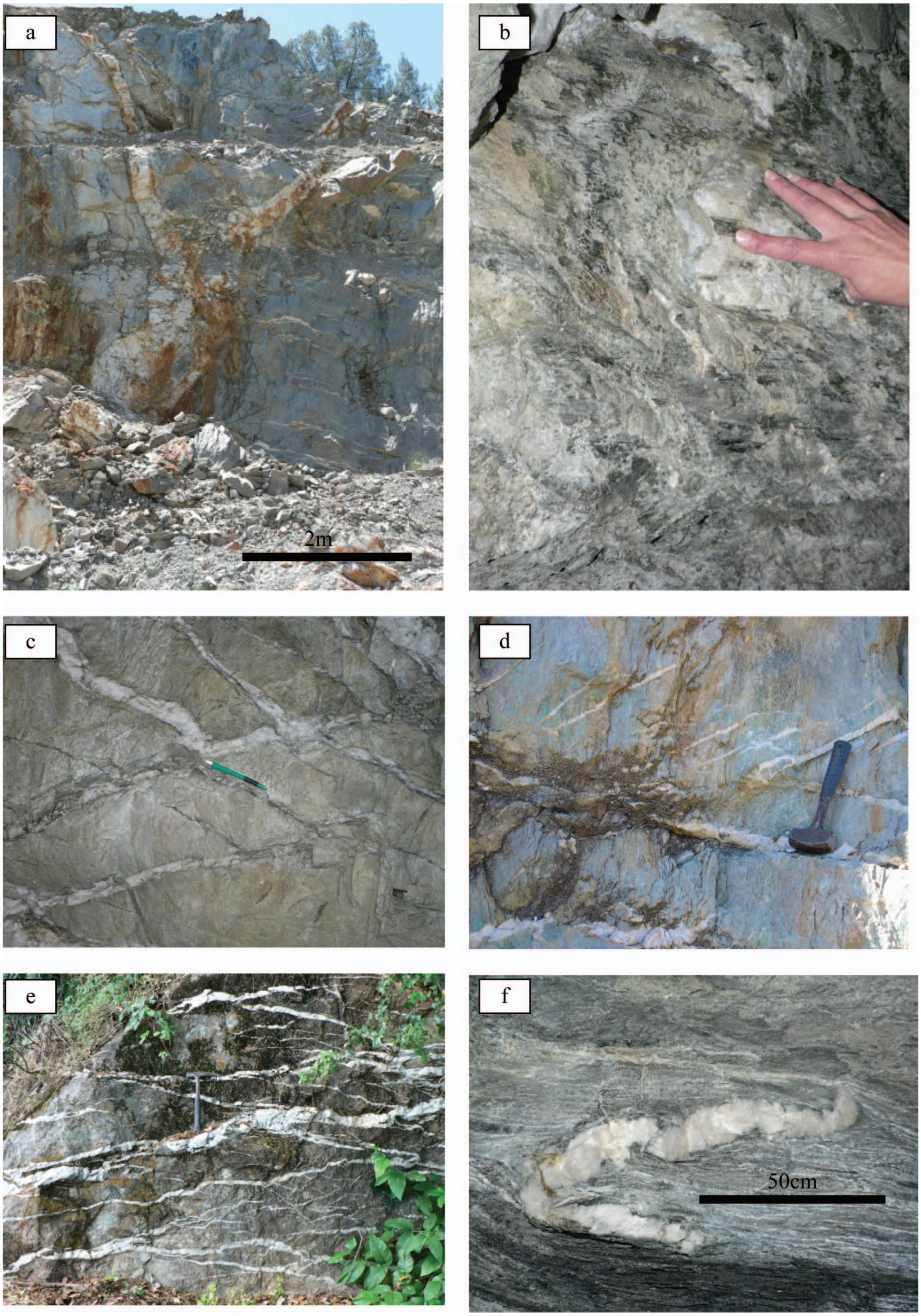
a
2m
b
c
d
e
f
50cm

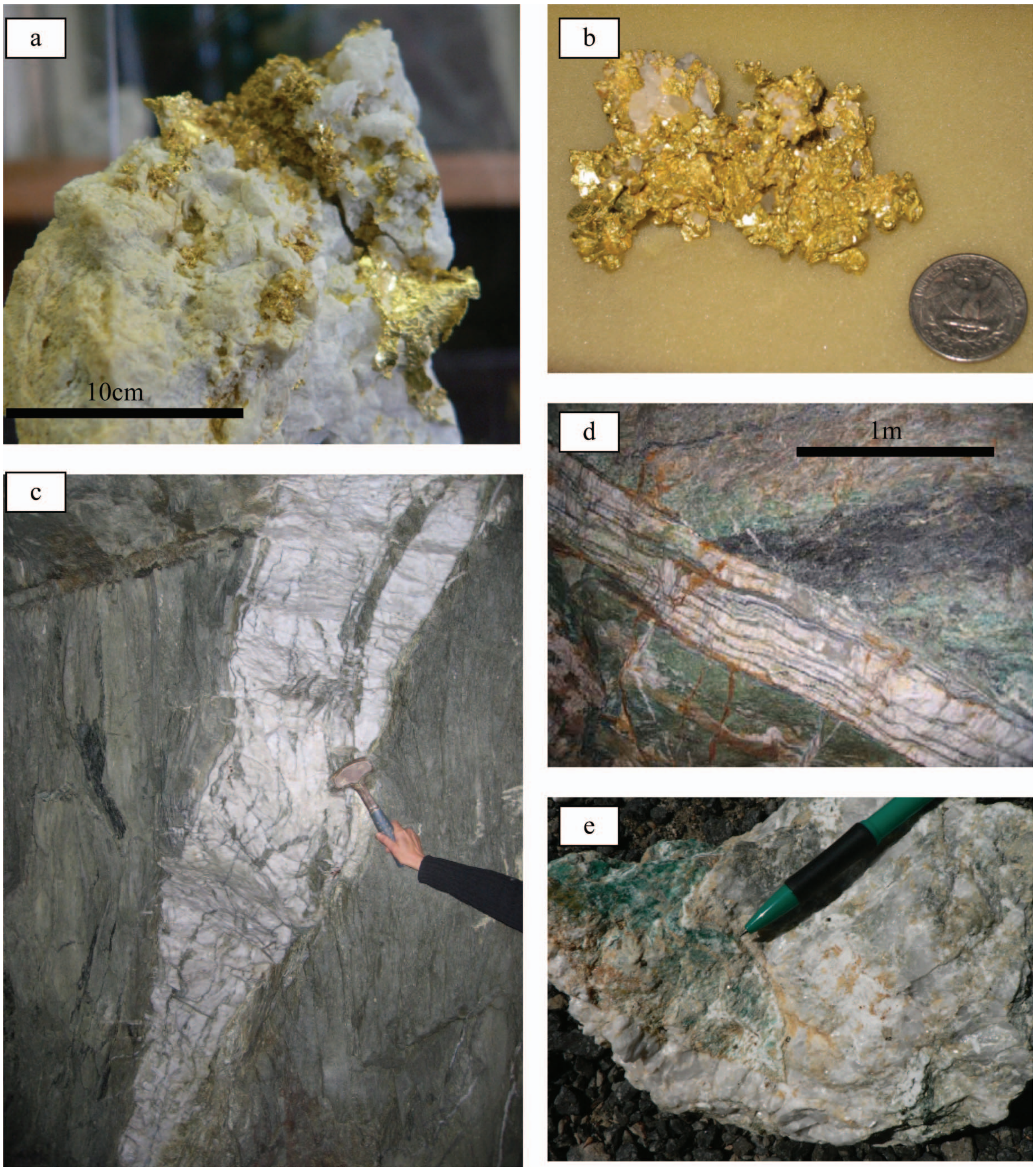

Figure 5 (a) High-grade ore specimen from the Harvard Pit, Jamestown (specimen kindly provided by R. Grunewald). (b) Quartz-gold nugget from the Sixteen-to-One deposit, Alleghany (specimen kindly provided by K. Testerman). (c) Reverse fault-hosted laminated to massive, stylolitic quartz vein (#42) cutting across the (near-vertical) foliation in phyllite in Sutter Creek deposit; the teeth in the chloritic stylotites define an east–west trend (approximately parallel to the orientation of the arm holding the hammer). (d) Laminated crack–seal vein in mariposite-altered serpentinite in the Sixteen-to-One deposit, Alleghany. (e) Quartz–feldspar–ankerite–mariposite vein with pyrite porphyroblasts from the Tittletown deposit, Jamestown district.

metamorphic origin of the ore-bearing fluids (Jia *et al.* 2003).

Accepting the *ca* 125–115 Ma interval as the main period of gold-bearing quartz-vein formation, the timing of mineralisation in the Sierra Nevada Foothills Metamorphic Belt would correspond to a significant change in accretionary dynamics along the North American plate margin during the Late Jurassic and Early Cretaceous (Tobisch *et al.* 1995). Studies by Glazner (1991) and Beck & Housen (2003) demonstrated that the absolute rate of convergence between the North American and Farallon Plates decreased in the Late Jurassic, with left-lateral tangential convergence (due to the North American Plate moving northwest) probably inducing predominantly northwest–southeast-oriented stress on the structural grain of the Sierra Nevada Foothills Metamorphic Belt. A relatively abrupt shift to primarily normal (east–west) convergence at about

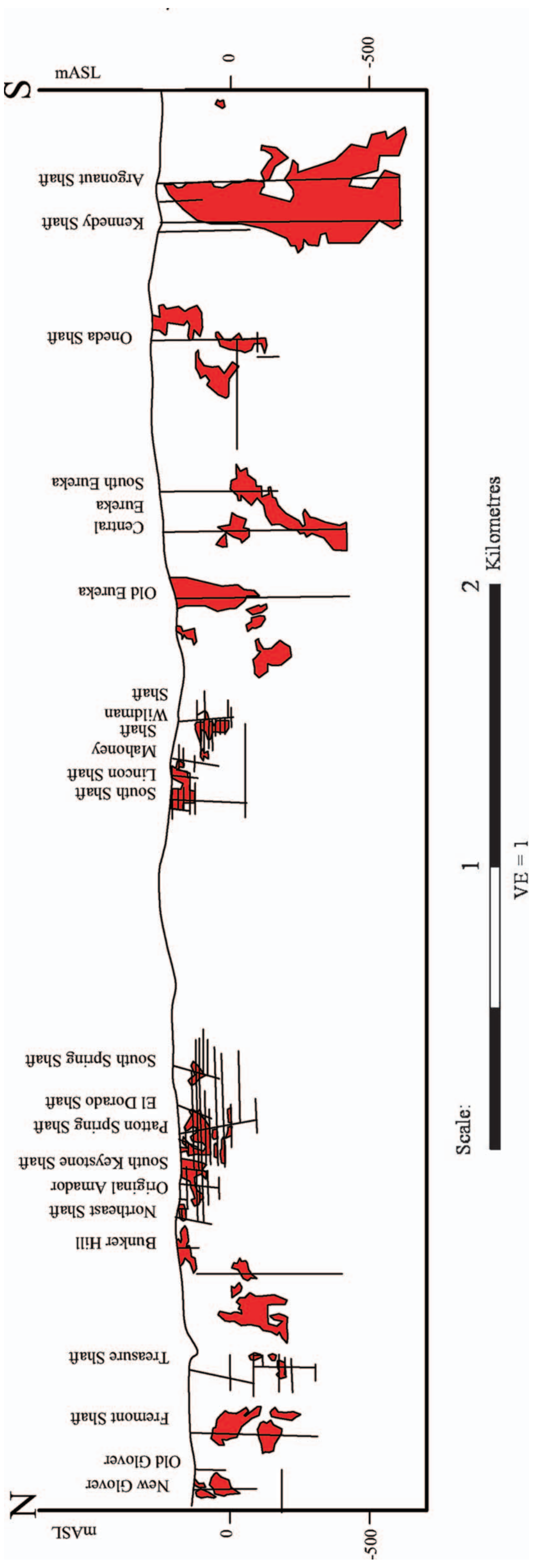

Figure 6 Longitudinal section of mined stopes in the Jackson-Plymouth district with average grades exceeding 5 g/t; the steeply northward plunge of the majority of stoped out ore

120 Ma, coupled with a subsequent increase in the sum rate of plate convergence, would have given rise to transpressional reactivation of major structures within the Sierra Nevada Foothills Metamorphic Belt, and the preferential development of dilational zones along misaligned segments of these and subordinate thrust faults. Efficient fluid focusing as part of this deformational regime occurred at a variety of scales, corresponding to structurally permeable zones within first-, second-, and third-order structures.

CONSTRUCTION OF A GIS FRAMEWORK FOR THE SIERRA NEVADA FOOTHILLS METAMORPHIC BELT

Traditional assessments of the endowment and fertility of metallogenic provinces rely heavily on field-based observations and interpretations. In addition to the mainly intra-deposit- to camp-scale field observations and structural interpretations outlined above, province-scale spatial relationships, when placed in the context of the tectonic evolution of the Sierra Nevada Foothills Metamorphic Belt, allow for the construction of a regionally consistent GIS framework for the Sierra Foothills gold province. This framework can then be interpreted in terms of a prospectivity assessment.

Due to the regional scale of this investigation, a variety of disparate data sources (Clark 1992; Saucedo *et al.* 2000; Snow & Scherer 2006) of varying density were compiled into broadly consistent empirical and derived layers of solid geology, structural elements, deposit locations, magnetics and gravity (Bouguer anomaly and isostatic residual gravity). Uncertainties and discrepancies in production figures, deposit names and location of the ~7000 mines contained in published datasets (Long *et al.* 1998; Frank 1999; Anonymous 2006) were considerably reduced via the compilation of a gold production and attribute database that contained 1248 significant mines (>150 kg Au produced), of which 813 were gold-bearing quartz-vein deposits (Northover 2006). The database was further refined via cross-referencing of deposits with data in Ferguson & Gannett (1932), Clark & Lydon (1962), and Clark (1992), separation of placer from lode-gold occurrences, and ground-proofing and validating their respective locations in a GPS-based framework. In many instances, actual production was obtained from the recalculation of published 'total value of production' figures using an average price of US$20.67 per ounce over the mine life, which corresponds with the fixed price of gold prior to 1932 (Clark 1992). Although introducing a level of uncertainty, this assumption is considered valid as ~85% of the total gold production from the Sierra Nevada Foothills Metamorphic Belt occurred pre-1932. Post-1932 mining economics dictated that the majority of the remaining 15% of total gold production was sourced from larger operations, for which complete production records exist, thereby further reducing uncertainty (Walker 2001).

In order to assess geological parameters critical to the localisation of gold mineralisation, solid geology and structural geology layers were constructed. Additional empirical inputs included magnetic and gravity

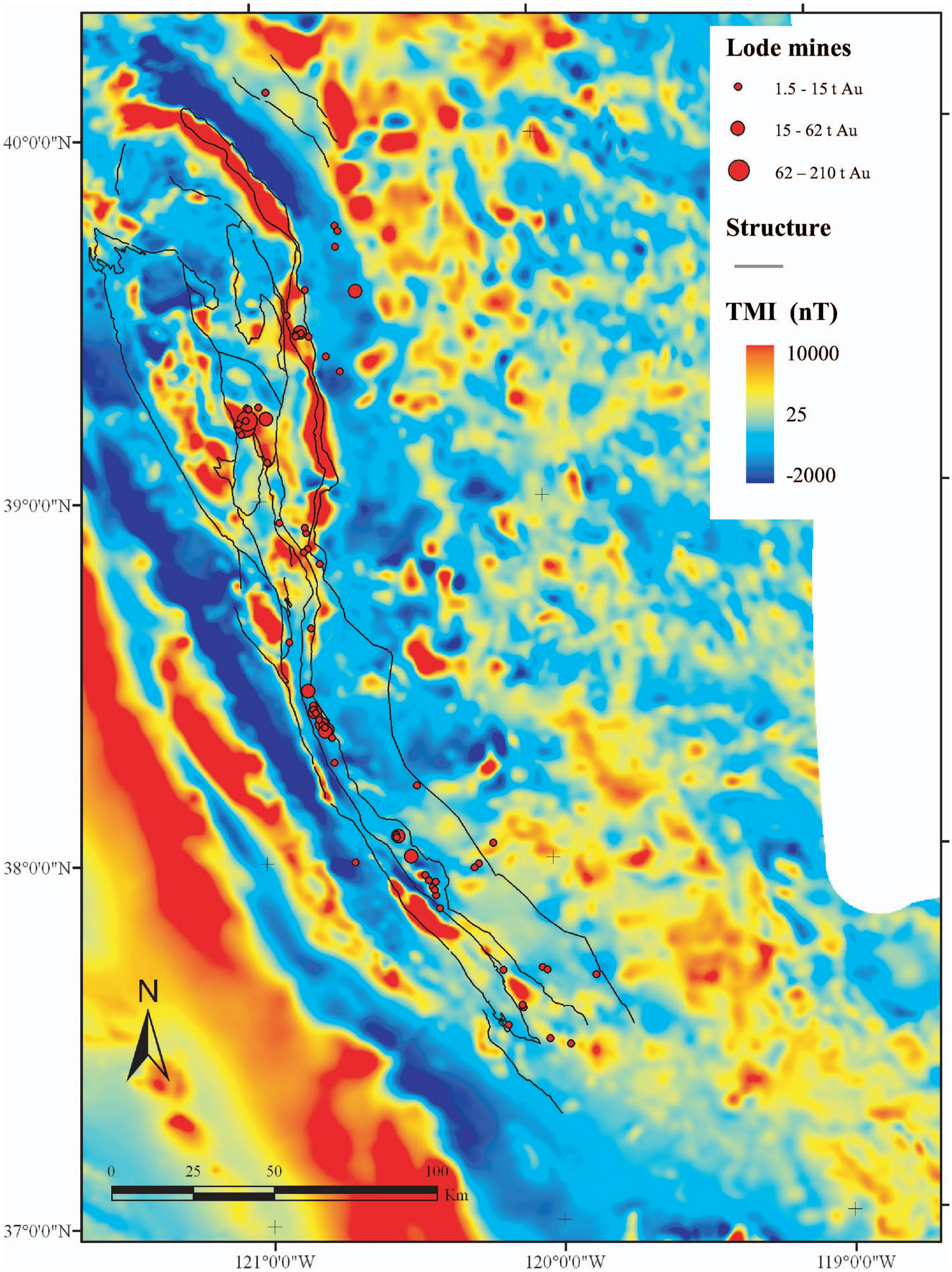

Figure 7 Total magnetic intensity pseudocolour representation of the Sierra Nevada Foothills Metamorphic Belt (standard deviation stretch, $n = 2$), with significant lode-gold deposits and first- and second-order faults in the northern and central portion of the belt superimposed (data from Ferguson & Gannett 1932; Clark & Lydon 1962; Clark 1992; Long *et al.* 1998; Frank 1999; Saucedo *et al.* 2000; Bankey *et al.* 2002; USGS 2002, 2006).

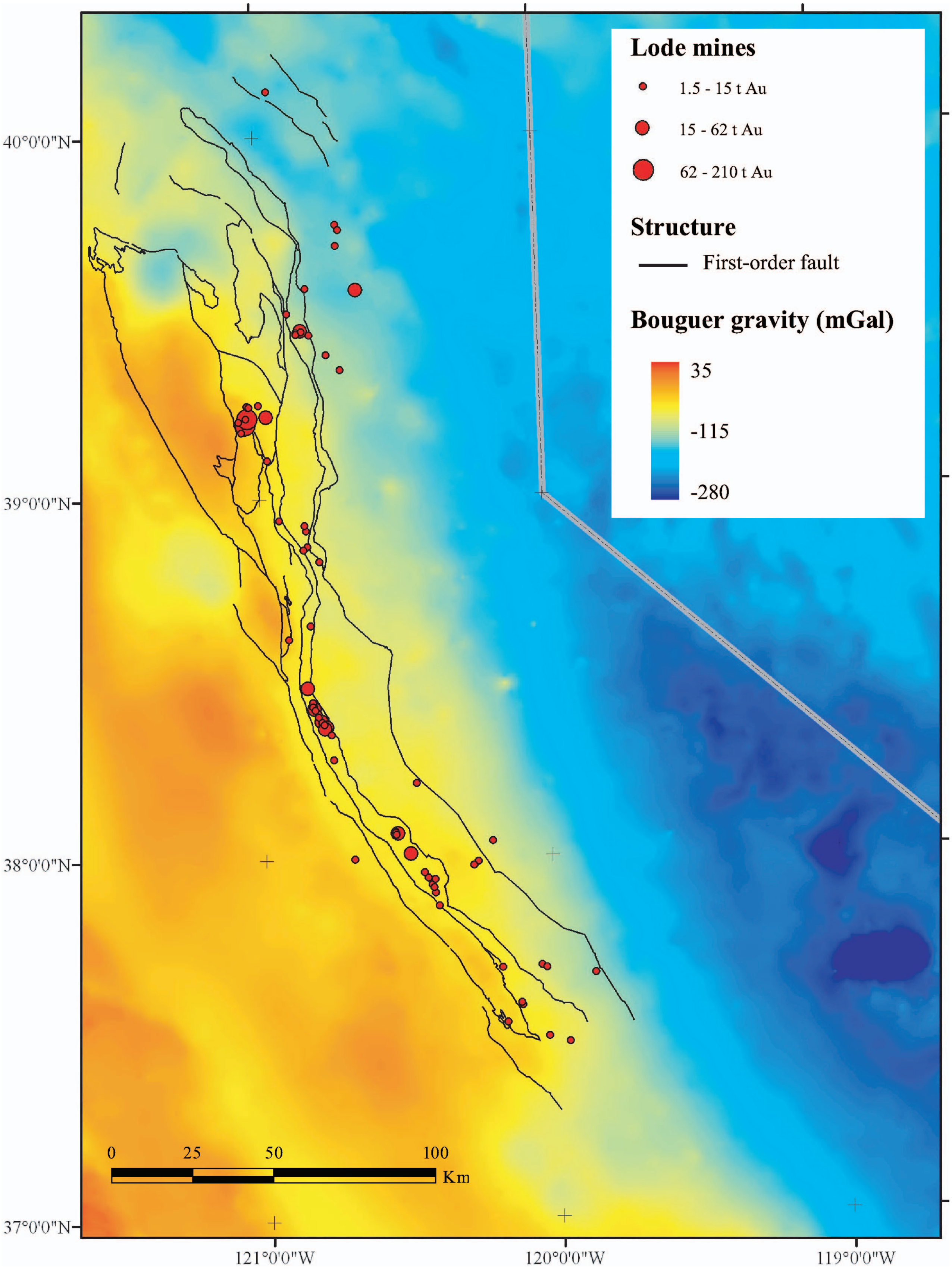

Figure 8 Pseudocolour representation of the constructed Bouguer gravity layer for the Sierra Nevada Foothills Metamorphic Belt, with significant lode-gold deposits and first- and second-order faults in the northern and central portion of the belt superimposed (data from Ferguson & Gannett 1932; Clark & Lydon 1962; Clark 1992; Long *et al*. 1998; Frank 1999; Saucedo *et al*. 2000; Bankey *et al*. 2002; USGS 2002, 2006).

data from Roberts & Jachens (1999) and the US Geological Survey (Bankey *et al.* 2002; USGS 2002, 2006). From these empirical layers, other empirical/ conceptual-derived layers such as distance to nearest fault or lithological contact could then be derived (Groves *et al.* 2003). Prior to digitising the geology and structural layers, the magnetic and gravity layers were used to interpret and cross-validate areas with limited and/or conflicting information. Two separate magnetic layers were interpolated, providing different resolution. The high-resolution layer was derived from data acquired from four separate aeromagnetic surveys, with line spacings of <1 km and sampling distances of <50 m (Roberts & Jachens 1999; USGS 2002). Although detailed, the area covered by these high-resolution surveys was less than one-third of the area of interest. Thus, a lower-resolution magnetic layer was interpolated to a cell resolution of 250×250 m from a Total Magnetic Intensity (TMI) dataset consisting of 246 000 points on a 1×1 km grid across the entire Sierra Nevada Foothills Metamorphic Belt (Bankey *et al.* 2002) (Figure 7). A Bouguer gravity anomaly layer, covering the entire length of the Sierra Nevada Foothills Metamorphic Belt (USGS 2006), was interpolated from 26 762 points using kriging techniques (Figure 8). Because isostatic residual gravity data were unavailable at the same resolution as the Bouguer gravity anomaly layer, an ArcMap interchange coverage was utilised (Kucks 1999). To avoid misalignment between the two gravity layers, the isostatic residual gravity layer was re-sampled by bilinear interpolation to the same resolution as the magnetic and Bouguer gravity anomaly layers (Northover 2006).

Lithologically disparate units in each terrane were grouped into six general lithotypes based on georeferenced input data in Saucedo *et al.* (2000), Irwin (2003), Day & Bickford (2004) and Snow & Scherer (2006). These included: sedimentary rocks, mixed volcanic and sedimentary rocks, volcanic rocks, granitoids, gabbros and diorites, and ultramafic rocks (cf. Figure 1). The structural layer (cf. Figures 7, 8) incorporates all terrane-bounding (first-order) and major intra-terrane faults recorded in georeferenced maps of Saucedo *et al.* (2000), Irwin (2003) and Snow & Scherer (2006). Higher-order structures are poorly represented, in part due to the scale of the study, but also because many are not recorded in existing datasets, particularly where they coincide with lithological boundaries. Where such structures are shown in Saucedo *et al.* (2000), they are extrapolated with the aid of the high-resolution TMI layer, which was also used to cross-validate the solid geology and structural layers.

COMPUTER-BASED ASSESSMENT OF CONTROLS ON GOLD MINERALISATION

Utilising the empirically derived layers described above, some of the geological and spatial controls on the distribution and size of gold deposits throughout the Sierra Foothills gold province can be examined in a GIS framework. These controls also represent quantifiable proxies for fluid source(s), transport pathways and efficient traps within a conceptual mineral systems framework. Whereas specific gold sources remain undefined, abundant primitive mafic rocks throughout the Sierra Nevada Foothills Metamorphic Belt are the most likely sources of significant volumes of ore constituents (Bierlein *et al.* 2006a). An empirical proxy for the genetic link between orogenic-gold formation,

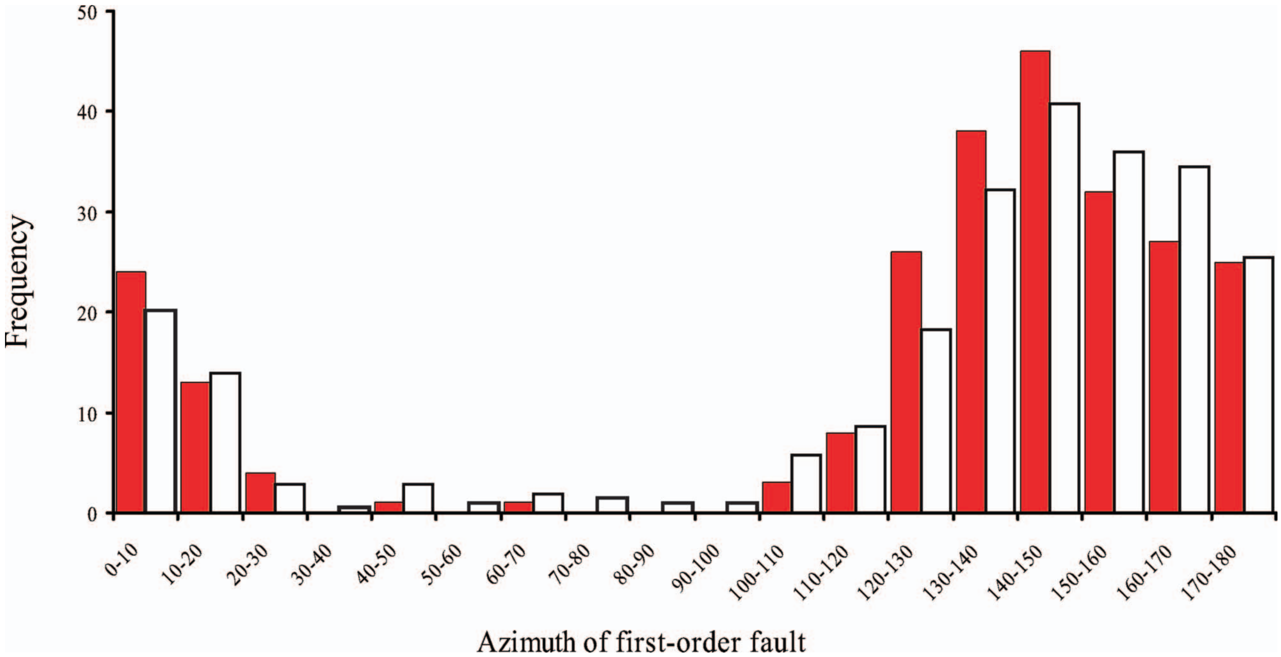

Figure 9 Relationship between the azimuth of the nearest first-order fault to significant lode-gold deposits in the northern and central Sierra Nevada Foothills Metamorphic Belt (solid bars). For comparison, the frequency distribution of the azimuth of all first-order faults (open bars) is also shown, illustrating the preferred spatial association of lode-gold deposits with misaligned fault segments.

accretionary processes and crustal shortening is the close spatial relationship between orogenic-gold deposits and first-order structures (i.e. transport pathways: Goldfarb *et al*. 2001). This relationship is based on the ability of transcrustal faults to enhance the efficient channelling of ore-bearing fluids from their source to shallower crustal levels (Groves *et al*. 2000). This spatial link is illustrated by the occurrence of ~75% of gold deposits within 4.5 km of such faults in the Mother Lode Gold Belt (90% within 8.6 km) in the central portion of the Sierra Nevada Foothills Metamorphic Belt. With the exception of deposits in the Grass Valley district, almost all gold deposits display a spatial affinity with the Melones Fault. At a crustal scale, the majority of major lode-gold deposits (production >1.5 t Au) in the Sierra Nevada Foothills Metamorphic Belt also occur within a narrow north-northwest-trending region that is marked by a strong gradient on a Bouguer gravity anomaly map of the western United States (USGS 2006), indicative of a significant change in crustal thickness and/or composition across this gradient (Figure 8).

As illustrated above, sites of gold deposition at district- to deposit-scale correlate well with the occurrence of both dilational and compressive jogs along first-order structures throughout the Sierra Nevada Foothills Metamorphic Belt (as well as in analogous settings elsewhere: Cox *et al*. 2001). Plotting the azimuth of the nearest first-order fault to significant gold deposits (Figure 9) highlights the coincidence of major gold deposits and segments of these faults that have an orientation notably different (≥15°) from that of the overall regional trend (~154°). A similar pattern emerges when, more locally, correlating the siting of major gold deposits along the Melones Fault with variations in the trend of this most significant of all first-order structures in the Sierra Nevada Foothills Metamorphic Belt (Figure 10). The best-endowed district in the Mother Lode Gold Belt, Jackson-Plymouth appears to contradict this pattern as it occurs proximal to a segment of the Melones Fault trending 156°, but the district is situated at the nose of a misaligned, restraining jog (assuming an east–west orientation of

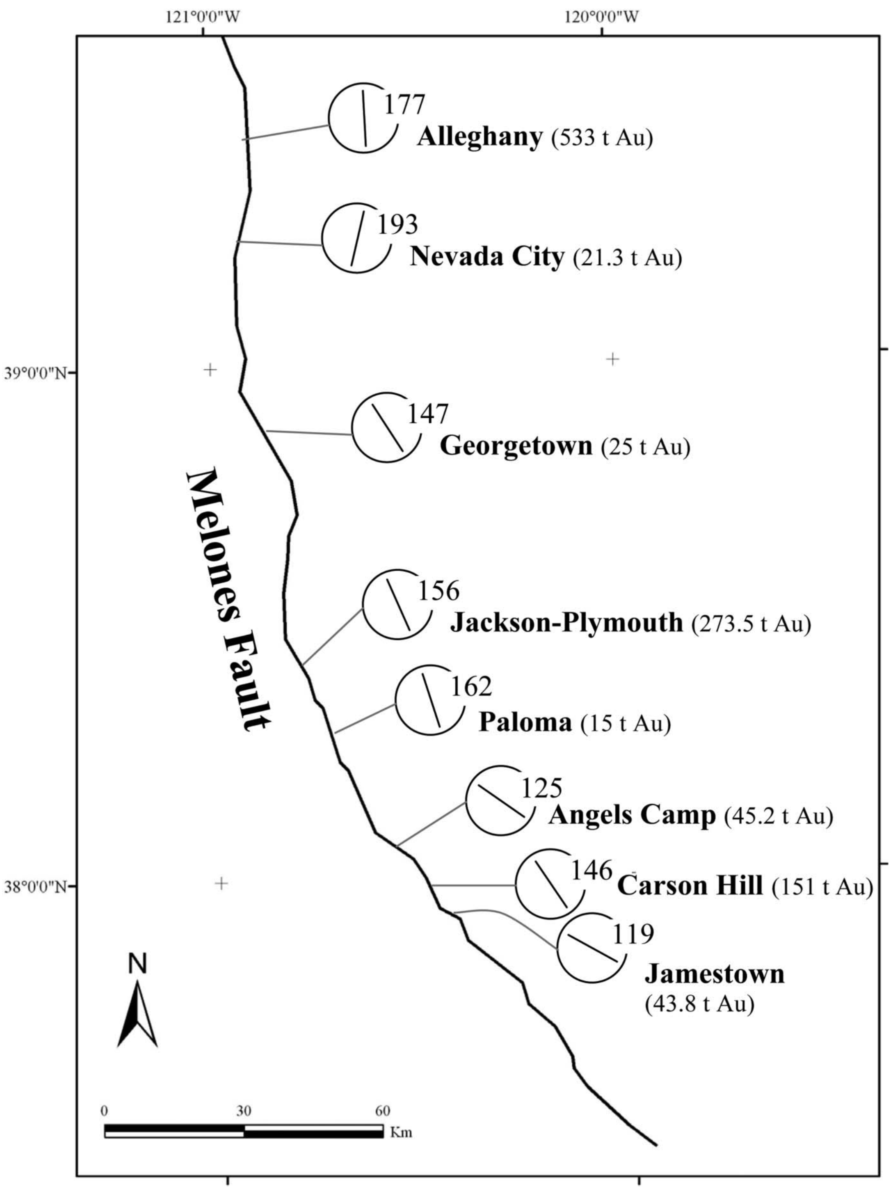

Figure 10 Spatial relationship of gold districts with misaligned segments (redrawn at 2.5 km intervals) of the first-order Melones Fault.

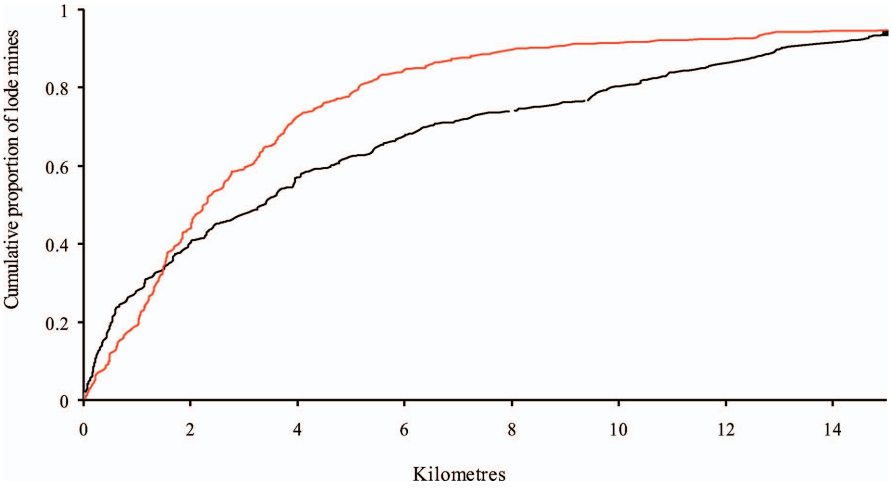

Figure 11 Cumulative production from significant lode-gold deposits in the northern and central portion of the Sierra Nevada Foothills Metamorphic Belt *vs* distance from the nearest first- (light-coloured line), and second- and third-order (black line) faults.

the far-field compressional regime), with the second-most productive district (Carson Hill) corresponding with a segment trending 146°. Similar relationships between the siting of major orogenic-gold deposits (and camps) and misaligned segments of major faults have been documented for the Eastern Goldfields Province in the Archean Yilgarn Carton of Western Australia by Hodkiewicz *et al.* (2005) and Weinberg *et al.* (2005). Interrogation of the solid and structural layers shows that both the Alleghany and Grass Valley districts occur within step-over jogs between two major (first-order) faults that are significantly misaligned relative to the overall regional trend (Figure 3).

Stepping down in scale, fluid focusing at the deposit-scale generally follows increased structural permeability into second- and third-order structures (Sibson & Scott 1998; Cox *et al.* 2001). On the basis of deposit-scale GIS analysis, Groves *et al.* (2000) argued that the interplay between second- and third-order structures is one of the most important aspects in determining the actual site of ore deposition. However, only 35% of the gold deposits in the Sierra Nevada Foothills Metamorphic Belt correlate with second- and third-order faults as the most proximal structure (Figure 11). The most probable cause for this low correlation is not the lack of a spatial relationship, but rather the inadequacy of the structural layer in terms of definition of higher-order faults. By contrast, many of the gold deposits display a strong spatial affinity to regions of magnetic gradients, and ~90% occur within 2 km of a lithological contrast in terms of the broad lithotypes defined in Figure 1 (Figure 12). These correlations strongly support the notion that many (mapped) lithological contacts, representing zones of significant competency gradients, particularly where serpentinite is juxtaposed with a felsic intrusion or sedimentary rock, are in fact faults. If this assumption is correct, it further emphasises the importance of rheological and permeability contrast in focusing fluid flow and controlling ore deposition. To test this notion, the relationship of orogenic-gold deposits and the azimuth of nearby (<3.5 km) lithological contacts was assessed. Figure 13 shows a preference of gold deposits towards contacts that strike between 140 and 150° (as opposed to the expected preferred regional trend of between 150 and 160°) and, as such,

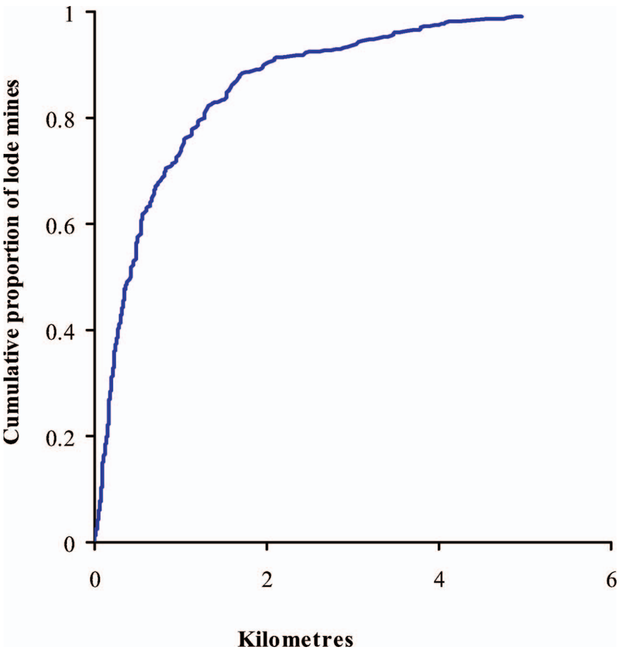

Figure 12 Cumulative production from significant lode-gold deposits in the northern and central portion of the Sierra Nevada Foothills Metamorphic Belt *vs* distance from the nearest lithological contrast.

probably represent dilational zones within misaligned segments of structural contacts. Thus, this is similar to the spatial correlation expressed at the scale of first-order faults.

Based on the lithotype classification undertaken in this study, the amount of gold produced from each of the six lithotypes in the Sierra Nevada Foothills Metamorphic Belt (normalised by area) can be quantified (Figure 14). Although the epigenetic nature of the deposits implies that host lithology is secondary, there is a strong preference towards volcanic rocks in terms of gold production (kg/km^2). Production from deposits in such volcanic rocks (95.3 kg/km^2) is significantly greater than that from deposits in mixed sedimentary and volcanic rocks (40.7 kg/km^2) and sedimentary rocks (37.3 kg/km^2). Production from deposits hosted in granitoids (11.4 kg/km^2), gabbros (16.8 kg/km^2), and

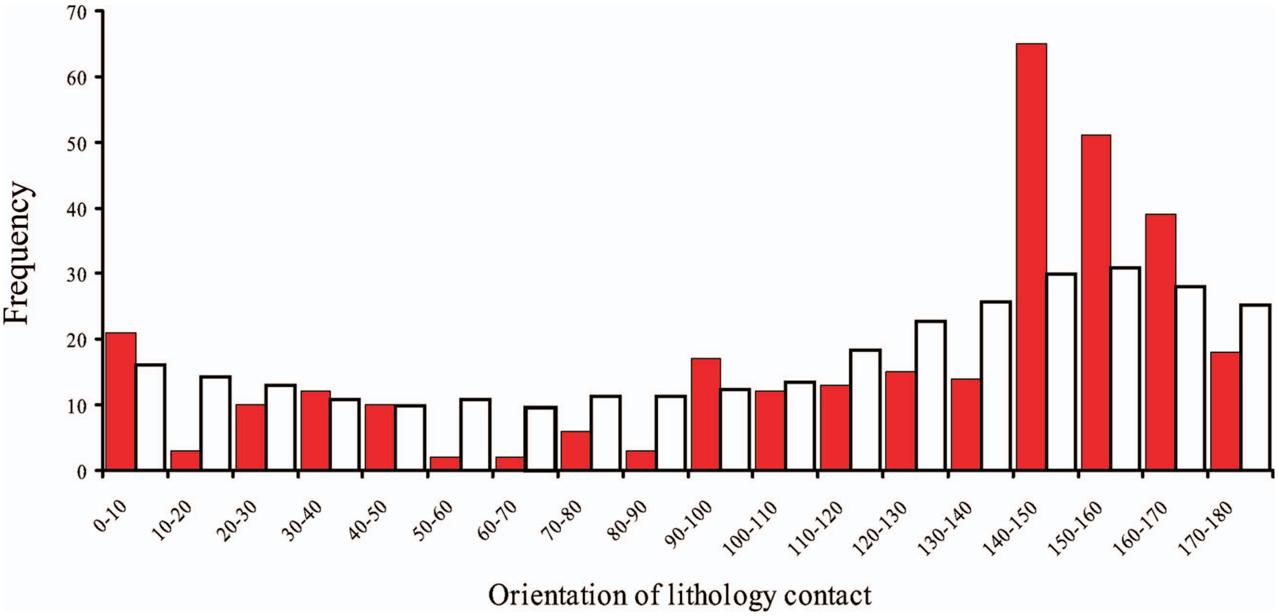

Figure 13 Relationship between the strike orientation of the nearest (mapped) lithological contact within 3.5 km to significant lode-gold deposits in the northern and central Sierra Nevada Foothills Metamorphic Belt (solid bars). For comparison, the frequency distribution of the azimuth of all mapped contacts (open bars) is also shown.

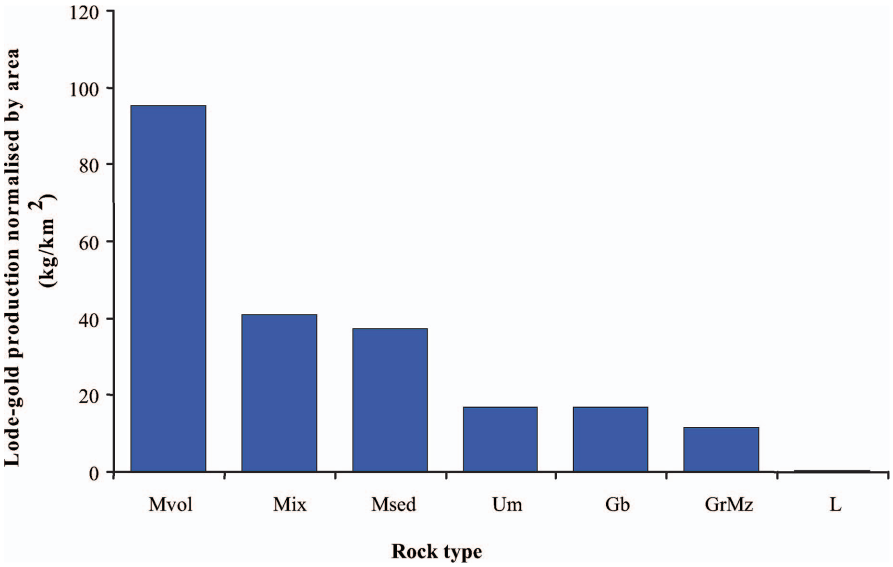

Figure 14 Comparison of host-rock type (based on the lithotype layer employed in this study) *vs* production of gold from lode-gold deposits (in kg/km^2). Mvol, volcanic rocks including greenstone, andesite – rhyolite flows, dacite, tuff, minor diabase and pillow lavas; Mix, mixed sedimentary and volcanic rocks, including slate, quartzite, hornfels, chert, phyllite, mylonite schist, gneiss and minor pyroclastic rocks; Msed, sedimentary rocks including sandstone, shale, chert, quartzite, slate and conglomerate; Um, ultramafic rocks (predominantly serpentinite); Gb, gabbro and dioritic rocks; GrMz, granite, quartz monzonite, granodiorite and quartz diorite; L, limestone.

ultramafic rocks (16.8 kg/km^2) is notably lower. The ultimate cause of this preference for gold deposits to be hosted by volcanic rocks is unclear but is probably related to a combination of chemical reactivity, rheological properties, and depositional/structural environment. The GIS analysis also confirms that there is no consistent spatial relationship between gold deposits and granitoids in the Sierra Foothills gold province.

A final test involved the efficiency of spatial parameters (first-order faults; second- and third-order faults; lithological contacts) in capturing significant known lode-gold deposits by using buffers of increasing size. By doing so, the portions of total area encompassed can be compared with the total cumulative portion of significant lode-gold deposits contained within this area, and the relative spatial relationship measured. Figure 15 shows that first-order structures represent the most efficient spatial proxy, followed by lithological contacts, and then second- and third-order faults. The result is likely to reflect the relatively

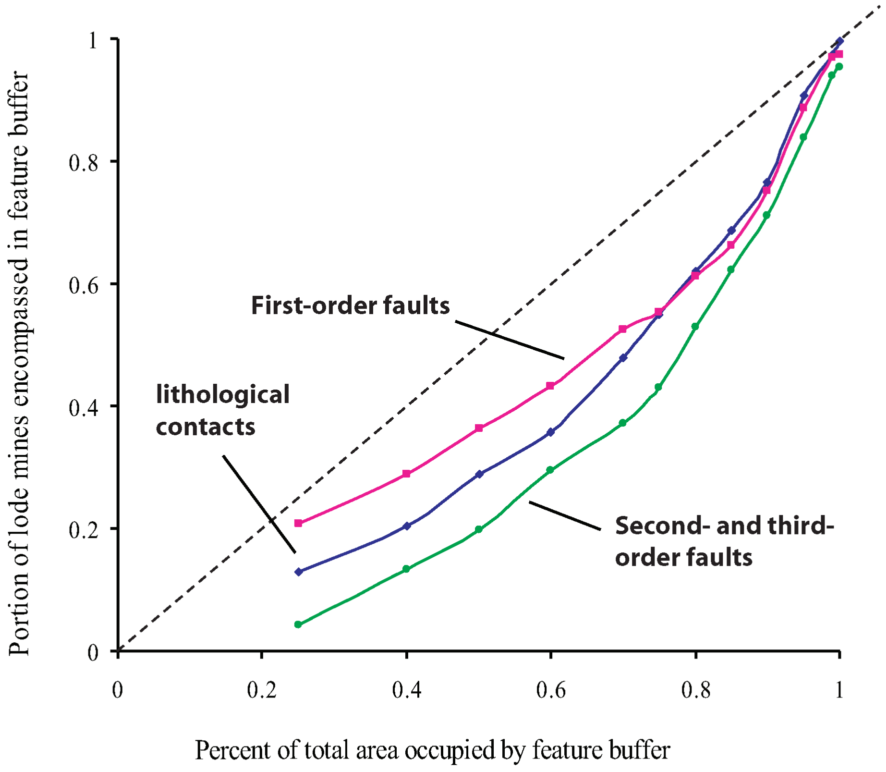

Figure 15 Relative buffer size of conceptual parameters (first-order faults; second- and third-order faults; lithological contacts) *vs* the percentage of known lode-gold mines in the northern and central Sierra Nevada Foothills Metamorphic Belt captured by the respective buffer, illustrating the apparent comparative efficiency of each parameter.

higher spatial density of first-order faults and (mapped) lithological contacts at the belt-scale, when compared with the number of second- and third-order faults clearly represented in available map data, rather than a true representation of the relative importance of the relationships.

SUMMARY AND CONCLUSIONS

The effectiveness of spatial parameters in identifying province-scale prospective areas is undoubtedly dependent on input data density. Lack of complete datasets, limited geochronological constraints, unreliable records (e.g. production), and insufficient spatial resolution all introduce uncertainties that severely limit the capability of any GIS-based analysis to determine and rank potentially prospective areas. This realisation is particularly important in the Sierra Foothills gold province, where most map data are old and inconsistent, and there are no continuous high-density geophysical datasets. Nevertheless, this study confirms conceptual and empirically established findings regarding the importance of certain geological and structural parameters in controlling the spatial distribution, abundance and size of orogenic-gold deposits. These parameters include proximity to first order; terrane-bounding structures; spatial affinity with misaligned fault segments that generate dilational or compressional jogs; lithological contacts with strong rheological contrasts; and regions characterised by geophysical (such as magnetic-intensity and/or gravity) gradients, as also shown, for example, in the Eastern Goldfields Province of the Yilgarn Craton, Western Australia (Bierlein *et al.* 2006b). In the Mother Lode belt, deposits are centred on north-northwest-trending gravity highs associated with the first-order Melones Fault. The majority of deposits are sited either within higher-order fault segments that parallel lithological contacts and trend $\geq 15^\circ$ from the regional, average orientation of $\sim 154^\circ$, or in jogs with misaligned cross-faults. On the basis of these findings and the successful identification of known gold deposits, basic GIS analysis has the potential to predict more highly prospective regions in this province. This approach, when combined with enhanced data density and high-quality input parameters, should prove equally successful when applied to exploration in analogous regions elsewhere.

ACKNOWLEDGEMENTS

We are grateful for generous in-kind support from Idaho-Maryland Mining and Sutter Creek Mine staff, as well as input by R. Wittkopp, R. Cortney, M. Payne, R. Grunewald, K. Testerman, R. Pease, J. Miller, K. Gessner, A. Hofstra and P. S. Peggy. We would also like to thank F. Pirajno and D. Arne for their reviews and comments. The US Geological Survey, the Centre for Exploration Targeting and the Tectonics Research Centre at the University of Western Australia, and the Australian Research Council (DP0342488 to FPB) are acknowledged for financial support.

REFERENCES

Albers J. P. 1981. A lithologic-tectonic framework for the metallogenic provinces of California. *Economic Geology* **76**, 765–790.

Anonymous 2006. Emgold Mining Corporation—Idaho-Maryland Project. Online <http://www.emgold.com/s/Idaho-Maryland_Project.asp>

BANKEY V., CUEVAS A., DANIELS D., FINN C. A., HERNANDEZ I., HILL P., KUCKS R., MILES W., PILKINGTON M., ROBERTS C., ROEST W., RYSTROM V., SHEARER S., SNYDER S., SWEENEY R., VELEZ J., PHILLIPS J. D. & RAVAT D. 2002. Digital data grids for the magnetic anomaly map of North America, North American Magnetic Anomaly Group (NAMAG). *US Geological Survey Open-File Report* **02-414**.

BARRIGA F. J. A. S., FYFE W. S., LANDEFELD L. A., MUNHA J. & RIBEIRO A. 1992. Mantle subduction: tectonic fluidization at depth. *Earth-Science Reviews* **32**, 123–129.

BATEMAN P. C. & EATON J. P. 1967. Sierra Nevada Batholith. *Science* **158**, 1407–1417.

BECK J. M. E. & HOUSEN B. A. 2003. Absolute velocity of North America during the Mesozoic from paleomagnetic data. *Tectonophysics* **377**, 33–54.

BIERLEIN F. P., ARNE D. C., BROOME J. & RAMSAY W. R. H. 1998. Metatholeiites and interflow-sediments from the Cambrian Heathcote Greenstone Belt, Australia: sources for gold mineralization in Victoria? *Economic Geology* **93**, 84–101.

BIERLEIN F. P., GROVES D. I., GOLDFARB R. J. & DUBÉ B. 2006a. Lithospheric controls on the formation of provinces hosting giant orogenic gold deposits. *Mineralium Deposita* **40**, 874–886.

BIERLEIN F. P., MURPHY F. C., WEINBERG R. F. & LEES T. 2006b. Distribution of orogenic gold deposits in relation to fault zones and gravity gradients: targeting tools applied to the Eastern Goldfields, Yilgarn Craton, Western Australia. *Mineralium Deposita* **41**, 107–126.

BÖHLKE J. K. 1999. Mother Lode Gold. *Geological Society of America Special Paper* **338**, 221–240.

BÖHLKE J. K. & KISTLER R. W. 1986. Rb–Sr, K–Ar, and stable isotope evidence for the ages and sources of fluid components of gold-bearing quartz veins in the northern Sierra Nevada foothills metamorphic belt, California. *Economic Geology* **81**, 296–322.

BROWN W. M., GEDEON D., GROVES D. I. & BARNES R. G. 2000. Artificial neural networks: a new method for mineral prospectivity mapping. *Australian Journal of Earth Sciences* **47**, 757–770.

CLARK W. B. 1992. Gold districts of California. *California Division of Mines and Geology Bulletin* **193**.

CLARK W. B. & LYDON P. A. 1962. Mines and mineral resources of Calaveras County, California. *California Division of Mines and Geology County Report* **2**.

COVENEY R. M. JR 1981. Gold quartz veins and auriferous granite at the Oriental mine, Alleghany, California. *Economic Geology* **76**, 2176–2199.

COX S. F., KNACKSTEDT M. A. & BRAUN J. 2001. Principles of structural control on permeability and fluid flow in hydrothermal systems. *Society of Economic Geologists Reviews* **14**, 1–24.

DAY H. W. & BICKFORD M. E. 2004. Tectonic setting of the Jurassic Smartville and Slate Creek complexes, northern Sierra Nevada, California. *Geological Society of America Bulletin* **116**, 1515–1528.

DILEK Y. D. & HARRIS R. 2004. Continental margins of the Pacific Rim: introduction. *Tectonophysics* **392**, 1–7.

EDELMAN S. H. & SHARP W. D. 1989. Terranes, early faults, and pre-Late Jurassic amalgamation of the western Sierra Nevada metamorphic belt, California. *Geological Society of America Bulletin* **101**, 1420–1433.

EVANS J. R. & BOWEN O. E. 1977. Geology of the southern Mother-Lode, Tuolumne and Mariposa Counties, California, California Division of Mines and Geology Map Sheet 36, Scale 1:24,000.

FERGUSON H. G. & GANNETT R. W. 1932. Gold quartz veins of the Alleghany district, California. *US Geological Survey Professional Paper* **172**.

FRANK D. G. 1999. An Arc/Info point coverage of mineral resource data system (MRDS) locations in eleven western states. *US Geological Survey Open-File Report* **99-169**.

GLAZNER A. F. 1991. Plutonism, oblique subduction, and continental growth: an example from the Mesozoic of California. *Geology* **19**, 784–786.

GOLDFARB R. J., GROVES D. I. & GARDOLL S. J. 2001. Orogenic gold and geologic time: a global synthesis. *Ore Geology Reviews* **18**, 1–75.

GOLDFARB R. J., PHILLIPS G. N. & NOKLEBERG W. J. 1998. Tectonic setting of synorogenic gold deposits of the Pacific Rim. *Ore Geology Reviews* **13**, 185–218.

GROVES D. I., GOLDFARB R. J., KNOX-ROBINSON C. M., OJALA J., GARDOLL S., YUN G. Y. & HOLYLAND P. 2000. Late-kinematic timing of orogenic gold deposits and significance for computer-based exploration techniques with emphasis on the Yilgarn Block, Western Australia. *Ore Geology Reviews* **17**, 1–38.

GROVES D. I., GOLDFARB R. J., ROBERT F. & HART C. J. R. 2003. Gold deposits in metamorphic belts: overview of current understanding, outstanding problems, future research, and exploration significance. *Economic Geology* **98**, 1–29.

HODKIEWICZ P. F., WEINBERG R. F., GARDOLL S. J. & GROVES D. I. 2005. Complexity gradients in the Yilgarn Craton: fundamental controls on crustal-scale fluid flow and the formation of world-class orogenic-gold deposits. *Australian Journal of Earth Sciences* **52**, 831–841.

IRWIN W. P. 2003. Correlation of the Klamath Mountains and Sierra Nevada: Sheet 1—map showing accreted terrains and plutons of the Klamath Mountains and Sierra Nevada, scale 1:1 000 000; Sheet 2—successive accretionary episodes of the Klamath Mountains and northern part of the Sierra Nevada. *US Geological Survey Open-File Report* **02-490**.

JIA Y., KERRICH R. & GOLDFARB R. J. 2003. Metamorphic origin of ore-forming fluids for orogenic gold-bearing quartz vein systems in the North American Cordillera: constraints from a reconnaissance study of δ^{15}N, δD, and δ^{18}O. *Economic Geology* **98**, 109–123.

JOHNSTON W. D. 1940. The gold–quartz veins of Grass Valley, California. *US Geological Survey Professional Paper* **194**.

KENTER K. B. 1998. The nature and timing of tectonism in the western facies terranes of Nevada and California—an outline of evidence and interpretations derived from geologic maps of key areas. *US Geological Survey Professional Paper* **1592**.

KISTLER R. W., DODGE F. & SILBERMAN M. L. 1983. Isotopic studies of mariposite-bearing rocks from the south-central Mother Lode, California. *California Geology* September 1983, 201–203.

KNOPF A. 1929. The Mother Lode System of California. *US Geological Survey Professional Paper* **157**.

KNOX-ROBINSON C. M. 2000. Vectorial fuzzy logic: a novel technique for enhanced mineral prospectivity mapping with reference to the orogenic gold mineralisation potential of the Kalgoorlie Terrane, Western Australia. *Australian Journal of Earth Sciences* **47**, 929–941.

KNOX-ROBINSON C. M. & GROVES D. I. 1997. Gold prospectivity mapping using a Geographic Information System (GIS) with examples from the Yilgarn Block of Western Australia. *Chronique de la Recherche Minière* **529**, 127–138.

KUCKS R. P. 1999. Bouguer gravity anomaly data grid for the conterminous United States. *US Geological Survey Digital Data Series* **DDS-9**.

LANDEFELD L. A. 1988. The geology of the Mother lode gold belt, Sierra Nevada Foothills metamorphic belt, California. *In*: Goode A. D. T., Smyth E. L., Birch W. D. & Bosma L. I. eds. *Bicentennial Gold 88*, pp. 167–172. Geological Society of Australia Abstracts **23**.

LINDGREN W. 1895. Characteristic features of California gold–quartz veins. *Geological Society of America Bulletin* **6**, 221–240.

LONG K. R., DEYOUNG J. H. & LUDINGTON S. D. 1998. Database of significant deposits of gold, silver, copper, lead, and zinc in the United States. *US Geological Survey Open-File Report* **98-206A**.

MILLER R. B. & PATERSON S. R. 1991. Geology and tectonic evolution of the Bear Mountains Fault Zone, Foothills Terrane, central Sierra Nevada, California. *Tectonics* **10**, 995–1006.

NELSON K. D., ZHU T. F., GIBBS A., HARRIS R., OLIVER J. E., KAUFMAN S., BROWN L. & SCHWEICKERT R. A. 1986. COCORP deep seismic reflection profiling in the northern Sierra Nevada, California. *Tectonics* **5**, 321–333.

NESBITT B. E. 1991. Phanerozoic gold deposits in tectonically active continental margins. *In*: Foster R. P. ed. *Gold Metallogeny and Exploration*, pp. 104–132. Blackie & Sons, Glasgow.

NORTHOVER H. 2006. An investigation into the controls on orogenic gold mineralisation in the Mother Lode Gold Province, California (USA). BSc(Hons) thesis, University of Western Australia, Perth (unpubl.).

PATERSON S. R. & WAINGER L. 1991. Strains and structures associated with a terrane bounding stretching fault: the Melones fault zone, central Sierra Nevada, California. *Tectonophysics* **194**, 69–90.

PAYNE M. & GRUNEWALD R. 2006. Mineral resource estimate Sutter Gold Project, Amador County, California. Sutter Gold Mining Inc.

ROBERTS C. W. & JACHENS R. C. 1999. Preliminary aeromagnetic anomaly map of California. *US Geological Survey Open-File Report* **99-440**.

ROSS D. C. 1983. Hornblende-rich, high grade metamorphic terranes in the southernmost Sierra Nevada, California, and implications for crustal depths and batholith roots. *US Geological Survey Open-File Report* **83-465**.

SAUCEDO G. D., BEDFORD D. R., RAINES G. L., MILLER R. J. & WENTWORTH C. M. 2000. GIS data for the geologic map of California. *California Department of Conservation, Division of Mines and Geology* CD-ROM 2000-007.

SHARP W. D. 1980. Ophiolite accretion in the northern Sierra. *EOS* **61**, 1122.

SHARRY J. 1982. Minimum age and westward continuation of the Garlock fault zone, Tehachapi Mountains, California. *Geological Society of America Abstracts with Program* **14**, 233.

SIBSON R. H. & SCOTT J. 1998. Stress/fault controls on the containment and release of overpressured fluids: examples from gold-quartz vein systems in Juneau, Alaska, Victoria, Australia and Otago, New Zealand. *Ore Geology Reviews* **13**, 293–306.

SNOW C. A. & SCHERER H. 2006. Terranes of the western Sierra Nevada Foothills Metamorphic Belt, California: a critical review. *International Geology Review* **18**, 46–62.

TOBISCH O. T., PATERSON S. R., SALEEBY J. B. & GEARY E. E. 1989. Nature and timing of deformation in the Foothill terrane, central Sierra Nevada, California: its bearing on orogenesis. *Geological Society of America Bulletin* **101**, 401–413.

TOBISCH O. T., SALEEBY J. B., RENNE P. R., MCNULTY B. & TONG W. 1995. Variations in deformation fields during development of a large-volume magmatic arc, central Sierra Nevada, California. *Geological Society of America Bulletin* **107**, 148–166.

USGS 2002. Digital aeromagnetic data sets of the Conterminous United States and Hawaii. *US Geological Survey Open-File Report* **02-361**. Online <http://pubs.usgs.gov/of/2002/ofr-02-361/>

USGS 2006. Geographic names information system (online). *US Geological Survey*. Online <http://geonames.usgs.gov/pls/gnispublic/>

VERNON R. H., PATERSON S. R. & GEARY E. E. 1989. Evidence for syntectonic intrusion of plutons in the Bear Mountain fault zone, California. *Geology* **17**, 723–726.

WALKER R. A. 2001. California's golden road to riches: natural resources and regional capitalism, 1848–1940. *Annuals of the Association of American Geographers* **91**, 167–199.

WEINBERG R. F., VAN DER BORGH P., BATEMAN R. & GROVES D. 2005. Kinematic history of the Boulder–Lefroy Shear System and controls on associated gold mineralization, Yilgarn Craton, Western Australia. *Economic Geology* **100**, 1407–1426.

WEIR R. H. & KERRICK D. M. 1987. Mineralogic, fluid inclusion, and stable isotope studies of several gold mines in the Mother Lode, Tuloumne and Mariposa Counties, California. *Economic Geology* **82**, 328–344.

WHITEHOUSE P. L., ENGLAND P. C. & HOUSEMAN G. A. 2005. A physical model for the motion of the Sierra Block relative to North America. *Earth and Planetary Sciences Letters* **237**, 590–600.

Received 14 February 2007; accepted 29 April 2007